

Effects of Poly(glycidyl ether) Structure and Ether Oxygen Placement on CO₂ Solubility

Caitlin L. Bentley, Tangqiumei Song, Benjamin J. Pedretti, Michael J. Lubben, Nathaniel A. Lynd,* and Joan F. Brennecke*

Cite This: *J. Chem. Eng. Data* 2021, 66, 2832–2843

Read Online

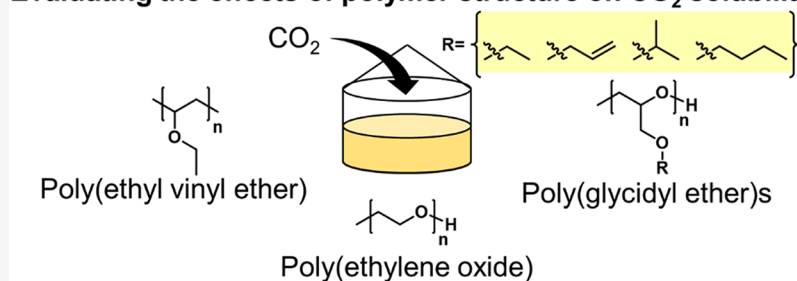
ACCESS |

Metrics & More

Article Recommendations

Supporting Information

Evaluating the effects of polymer structure on CO₂ solubility



ABSTRACT: The solubility of CO₂ in poly(ethylene oxide), poly(ethyl glycidyl ether), poly(*iso*-propyl glycidyl ether), poly(allyl glycidyl ether), poly(*n*-butyl glycidyl ether), and poly(ethyl vinyl ether) was measured at room temperature and 333.15 K and pressures up to 15 bar. CO₂ solubility, expressed as mole fraction in terms of molecular weight of the polymer repeat unit, was directly related to polymer repeat unit molecular weight regardless of pendant chain structure or ether oxygen placement in the backbone. The molality of CO₂ was highest in poly(ethyl vinyl ether) and was equal in all the poly(glycidyl ethers) and poly(ethylene oxide). The standard enthalpies and entropies of CO₂ absorption in poly(ethylene oxide), poly(ethyl glycidyl ether), and poly(ethyl vinyl ether) were calculated from the Henry's constants obtained from three isotherms. CO₂ dissolution was slightly more favorable enthalpically in poly(ethylene oxide). However, the entropic penalty for absorption was lower in poly(ethyl glycidyl ether) and poly(ethyl vinyl ether). These results suggest that poly(glycidyl ethers) and poly(ethyl vinyl ether) are promising alternatives to poly(ethylene oxide) for CO₂ separation by absorption or membrane separation because they have similar CO₂ uptake capacity, low glass transition temperatures, are amorphous, and are more hydrophobic than poly(ethylene oxide).

1. INTRODUCTION

Poly(ethylene oxide) (PEO) has been used for CO₂ separations as a liquid absorbent since the 1960s and was first applied in membrane applications in the late 1980s.^{1,2} Favorable quadrupolar interactions between the ether oxygens in the polymer backbone and dissolved CO₂ result in high solubility and permeability.^{3–6} Currently, PEO is used in two major industrial separations: (1) as the main component of Selexol, an industrial acid gas absorbent, and (2) the Polaris membrane, which is the first commercial membrane used for CO₂ separation.^{1,7} In the 50 years of the Selexol process, research interest in PEO for CO₂ separation has not declined. PEO has been cross-linked to make free-standing membranes^{3,4,8} and has been incorporated as a membrane additive^{4,9} or the soft-segment of block copolymer membranes to increase solubility.^{4,6} PEO has also been used as a nonaqueous cosolvent for amine and ionic liquid (IL) solutions to increase regeneration efficiency and reduce corrosion, energy consumption, and viscosity.^{10–12}

Despite its advantages, the application of PEO to CO₂ capture suffers from two main drawbacks: crystallinity and hydrophilicity. Gases are not soluble in crystalline domains.^{9,13} Carbon dioxide is affected more than other gases, leading to lower selectivity.⁹ Water vapor is a major component of flue gas; therefore, consistent material performance under humid conditions is important. However, water vapor decreases permeability,¹⁴ which could be the result of a decrease in solubility due to competitive sorption of water vapor.¹⁵

Crystallinity is managed in industrial applications by limiting the molecular weight of a continuous PEO chain. As a result, low molecular weight PEO can be used as an absorbent. In membrane applications, where a free-standing structure is

Received: March 22, 2021

Accepted: May 24, 2021

Published: June 2, 2021



Table 1. Nomenclature, Structure, Source, and Purity of the Materials Used in This Study^a

Abbreviation	Structure	Nomenclature	Source	Purity (wt %)
PEO-0.4		Poly(ethylene oxide)	MilliporeSigma	95
PEGE-5		Poly(ethyl glycidyl ether) ⁴	Synthesized	96
PiPGE-7		Poly(<i>iso</i> -propyl glycidyl ether) ⁴	Synthesized	95
PAGE-11		Poly(allyl glycidyl ether)	Synthesized	89
PnBGE-7		Poly(<i>n</i> -butyl glycidyl ether) ⁴	Synthesized	96
PEVE-2		Poly(ethyl vinyl ether)	MilliporeSigma	93
CO ₂		Carbon Dioxide, Instrument grade	Airgas	99.99

^aPurchased materials were used without further purification. The number in the abbreviation indicates the approximate number averaged molecular weight in kg/mol.

required, the molecular weight can be limited by cross-linking or copolymerization.^{4–6,8,14,16} Crystallinity can also be decreased by swelling with additives such as ionic liquids.^{17,18} Nonetheless, it may be advantageous to use higher molecular weight polymers, especially in membrane applications. Increasing molecular weight increases the permeability of CO₂ in PEO more than other gases, despite selectivity reaching an asymptote at 700 g/mol.¹⁹ As the molecular weight between cross-links in a membrane decreases, the cross-link density increases. Cross-link density has varied effects depending on polymer structure but is often found to decrease permeability owing to a reduction in chain flexibility.^{5,16}

In contrast to PEO, atactic poly(glycidyl ethers) are noncrystalline, hydrophobic, and have low glass transition temperatures, which are favorable for gas separation applications.²⁰ Because atactic poly(glycidyl ethers) do not crystallize, there is no limit on molecular weight, except that which is imposed by the synthesis. Although poly(glycidyl ethers) have not yet been widely applied to CO₂ capture, a recent study reports the permeabilities and solubilities of CO₂, N₂, and H₂ in copolymer membranes of PEO and poly(*n*-butyl glycidyl ether). Interestingly, these membranes show consistent performance under humidified conditions.²⁰ Poly(glycidyl ethers) can be used as liquid absorbents at any

temperature and molecular weight and can be incorporated into membranes in a similar manner to PEO, thus showing promise in CO₂ separation applications.

In this work, we explore the potential of a structurally homologous series of poly(glycidyl ethers) as alternatives to PEO for CO₂ separation applications. The CO₂ solubility was measured gravimetrically and is reported in terms of molality and mole fraction based on the molecular weight of the polymer repeat unit. To our knowledge, these are the first measurements of CO₂ solubility in non-cross-linked poly(glycidyl ethers). The effect of ether oxygen placement in the backbone and/or the polymer side chain was studied by comparing the CO₂ solubility in PEO, poly(ethyl glycidyl ether) (PEGE), and poly(ethyl vinyl ether) (PEVE). The standard enthalpy and entropy of absorption were determined for PEO, PEGE, and PEVE using Henry's constants for CO₂ at three temperatures. We also investigated poly(*iso*-propyl glycidyl ether) (PiPGE), poly(allyl glycidyl ether) (PAGE), and poly(*n*-butyl glycidyl ether) (PnBGE).

2. MATERIALS AND METHODS

2.1. Materials and Polymer Synthesis. All polymers used in this work were purchased from MilliporeSigma or were

synthesized according to previously published methods.^{21,22} The full name, abbreviation, structure, source, and purity are reported in Table 1. The purity was estimated by ¹H NMR spectroscopy performed on a 400 MHz Agilent MR spectrometer at room temperature and referenced to the residual solvent signal of CDCl₃. The detection limit of ¹H NMR spectroscopy was estimated as 1% by weight based on the peak height relative to the ¹³C satellite peaks. Any volatile impurities were removed by drying *in vacuo* of the bulk polymer samples after synthesis and purification and drying *in situ* before gas sorption measurements. Butylated hydroxytoluene (<1 wt %) was added to the bulk PAGE sample to suppress cross-linking, lowering its purity. The NMR spectra are shown in the Supporting Information (Figures S1–S6).

Three of the polymers were synthesized for a previous study.²³ The polymerization of poly(allyl glycidyl ether) proceeded as follows.

Synthesis of Poly(allyl glycidyl ether). Allyl glycidyl ether was dried over CaH₂ and degassed by three freeze–pump–thaw cycles. The anionic polymerization of allyl glycidyl ether was performed in custom, thick-walled glass reactors fitted with ACE thread adapters according to previously reported methods.^{21,22} The polymerization was carried out at 313.15 K to minimize allyl isomerization. The initiator, benzyl alcohol, was added via gastight syringe and was deprotonated by titration with potassium naphthalenide solution (0.3 M, THF). The polymerization was terminated with acidic methanol after the viscosity appeared constant. The resulting polymer was precipitated in hexanes and was dried *in vacuo*. The molecular weight was measured by size exclusion chromatography (SEC) using differential refractive index (RI) and multiangle light scattering (MALS) with $dn/dc = 0.0468$: $M_n = 11.3$ kg/mol, $M_w = 11.8$ kg/mol, $D = 1.04$. ¹H NMR (400 MHz, CDCl₃): δ 7.31 (multiplet, 4H, C₆H₅–CH₂–O–), δ 5.88ii (multiplet, 154H, –OCH₂CH=CH₂), δ 5.20 (doublet of doublets, 354iiH, –OCH₂CH=CH₂), δ 4.52z (singlet, 2H, C₆H₅–CH₂–O–), δ 3.97i (doublet, 350H, –OCH₂CH=CH₂), δ 3.64–3.43 (multiple overlapping, 878H, –CH₂CH–(CH₂OCH₂CH=CH₂)O–).

2.2. Size Exclusion Chromatography. Size exclusion chromatography (SEC) was used to determine polymer number- and weight-average molecular weight and dispersity. SEC was performed on one of two Agilent systems, both of which were equipped with a 1260 isocratic pump, degasser, and column chamber maintained at 303.15 K. System 1 contained Agilent PLgel 10 μ m MIXED-B and 5 μ m MIXED-C columns to measure molecular weights between 200 and 10 000 000 g mol^{–1} relative to polystyrene standards. System 2 contained an Agilent PLgel 10 μ m MIXED-B column to measure molecular weights between 500 and 10 000 000 g mol^{–1} relative to polystyrene standards. Chloroform with 50 ppm amylene and tetrahydrofuran were used as the mobile phases on systems 1 and 2, respectively. System 2 was additionally equipped with a suite of detectors from Wyatt Technologies. Multiangle light scattering (MALS) was measured using a DAWN HELEOS II Peltier system with differential refractive index (dn/dc [=] mL/g) measured with an Optilab TrEx and differential viscosity measured using a Viscostar II. The suite of detectors measured polymer concentration, molecular weight, and viscosity. SEC results are shown in Figures S7–S9 of the Supporting Information.

2.3. Thermal Analysis. Differential scanning calorimetry (DSC) was used to determine polymer melting points and

glass transition temperatures. It was performed on a TA Instruments TA250 under N₂ atmosphere. The glass transition temperature is reported from the third heating scan. Thermogravimetric analysis (TGA) was used to determine the onset temperature of polymer decomposition. It was performed on a Mettler Toledo DSC/TGA 3+ under N₂ atmosphere with a heating rate of 10 K/min. Thermal analysis results are shown in Figures S10–S13 of the Supporting Information.

2.4. Carbon Dioxide Absorption. The solubility of carbon dioxide in the liquid polymers was measured in a gravimetric gas sorption analyzer (IGA001 or IGA003, Hiden Isochema) shown in Figure 1. Sample sizes of 50–80 mg were

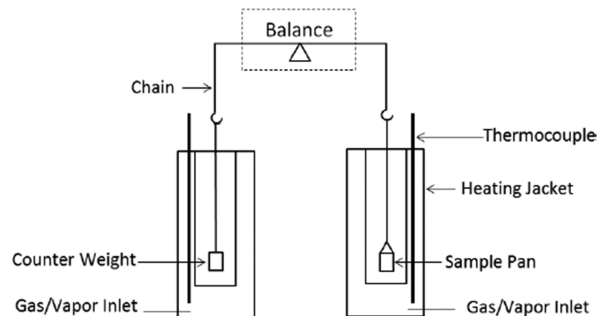


Figure 1. Schematic of the gravimetric gas sorption analyzer used in this work. Originally printed in reference 24.

used for the experiment. The uncertainty in the mass reading is ± 0.1 μ g. The system was evacuated at measurement temperature (bulk polymer samples were purified prior to removing samples for gas uptake²³) to remove residual volatile impurities overnight or until the sample mass was stable for at least 1 h, using a turbomolecular pumping station (TSH 071 with TC 110 controller, Pfeiffer Vacuum) to 10^{–6} mbar. Complete gas sorption isotherms were obtained by performing absorption and desorption cycles at each temperature. The temperature was maintained, for measurements above room temperature, with a recirculating bath (Neslab RTE 7 or LT ecocool 150). The gas uptake at each pressure was determined from the change in sample mass after applying a buoyancy correction.^{25,26} The uncertainty in the temperature measurement is ± 0.1 K and in the pressure reading is ± 0.01 bar. PEO swelling upon CO₂ dissolution below 20 bar is negligible.¹⁵ Therefore, polymer swelling due to gas dissolution was neglected in the buoyancy correction.

2.5. Density. Polymer densities were measured by one of three techniques. The most accurate measurements were obtained, when possible, using an oscillating U-tube Anton Paar 4500 densitometer. The estimated uncertainty in densitometer measurements is based on the estimated sample purities shown in Table 1.²⁷ Because PAGE is prone to cross-linking (even with stabilizer added), its density was not measured in the vibrating tube densitometer. Rather, the density at room temperature was measured by weighing a sample of known volume in triplicate. The estimated uncertainty of these measurements is $\pm 2.2\%$, based on the average relative deviation from the densitometer measurements for samples that could be measured both ways. The density of the PAGE at elevated temperature was measured using a buoyancy technique in the IGA using nitrogen because it is sparingly soluble in the polymers at low pressures. The

Table 2. Polymer Identity, Molecular Weight of Each Repeat Unit (MW RU), Number Averaged Molecular Weight (M_n), Polydispersity Index (PDI), Melting Temperature (T_m), Glass Transition Temperature (T_g), and Decomposition Onset Temperature (T_{onset})^a

polymer name	MW RU (g/mol)	M_n (kg/mol)	PDI	T_m (K)	T_g (K)	T_{onset} (K)
PEO-0.4	44	0.40 ± 0.03	1.26	294.15	204.15	642.15
PEGE-5	102	5.1 ± 1.2 ²³	1.98 ²³		209.15 ²³	643.15 ²³
PIPGE-7	116	7.0 ± 0.2 ²³	1.07 ²³		208.15 ²³	640.15 ²³
PAGE-11	114	11.3 ± 0.3	1.04		194.15 ²³	621.15 ²³
PnBGE-7	130	7.0 ± 0.2 ²³	1.07 ²³		194.15 ²³	643.15 ²³
PEVE-2	72	1.9 ± 0.3	1.60		213.15	609.15

^aStandard uncertainties are $u(T_m) = 1$ K, $u(T_g) = 1$ K, $u(T_{\text{onset}}) = 2$ K.

Table 3. Polymer Densities as a Function of Temperature^a

T/K	PEO-0.4	PEGE-5	PIPGE-7	PAGE-11	PnBGE-7	PEVE-4
295	1.127 ± 0.005	1.046 ± 0.004	0.999 ± 0.005	1.08 ± 0.05 ^b	0.987 ± 0.004	0.959 ± 0.007
313.15	1.113 ± 0.005					0.947 ± 0.007
333.15	1.097 ± 0.005	1.017 ± 0.004	0.970 ± 0.005	1.06 ± 0.02 ^c	0.960 ± 0.004	0.932 ± 0.007
343.15		1.009 ± 0.004				

^aAll measurements unless indicated otherwise were performed with the Anton Paar DMA 4500 Densitometer. Standard uncertainty is $u(T) = 0.1$ K except at room temperature, where $u(T) = 1.5$ K. ^bAverage of three measurements of weight of a sample with a known volume. ^cIGA buoyancy method measurement with nonsorbing gas.

estimated uncertainty in these measurements is ±4.5%, once again based on the average relative deviation from densitometer measurements for samples that could be measured both ways. A detailed description of the buoyancy technique to determine sample density can be found in the Supporting Information. The impact of uncertainty in the density measurements on CO₂ uptake and Henry's law constants is discussed in the Supporting Information (Figures S15 and S16).

2.6. Viscosity. Polymer viscosities were measured by one of three techniques. The polymer with the lowest viscosity, PEO-0.4, was measured in a rolling ball viscometer (Anton Paar Lovis 2000 M/ME) with an accuracy of 0.5%. The other polymers were measured using a Brookfield CAP2000 cone and plate viscometer (accuracy of 7%) or a Anton Paar SVM 2001 viscometer (accuracy of 0.5%).

3. THEORY AND CALCULATION

3.1. Henry's Law Constant. The Henry's law constant (H) of CO₂ dissolution in liquid polymers is described by eq 1 and was obtained from a linear fit of the gravimetric gas uptake isotherms on a molality (mol CO₂/kg polymer) and mole fraction basis.

$$H(T) = \lim_{x_i \rightarrow 0} \frac{P}{x_i} \quad (1)$$

Where, P is the partial pressure of CO₂ in bar, and x_i represents the molality of dissolved CO₂ or the mole fraction of CO₂ in the polymer calculated based on the molecular weight of the repeat unit, not the molecular weight of the polymer chain. The uncertainty in H calculated by propagation of the density uncertainty was always less than the linear regression uncertainty. Therefore, linear regression uncertainties are reported for all Henry's constants. In the case where multiple isotherms were measured at a single temperature, all data was used to calculate a single Henry's constant.

3.2. Thermodynamics of Gas Absorption. The relationship between the standard Gibbs free energy and the Henry's law constant is shown in eq 2. Combining this with the

definition of ΔG^0 shown in eq 3 indicates that the standard enthalpy and entropy of absorption can be obtained from the Henry's law constants at multiple temperatures by performing a weighted linear fit to $\ln\left(\frac{H}{P^0}\right)$ as a function of T^{-1} , where H is the Henry's law constant, P^0 is the standard state pressure, and T is the temperature (eq 4).

$$\Delta G^0 = RT \ln\left(\frac{H}{P^0}\right) \quad (2)$$

$$\Delta G^0 = \Delta H_{\text{abs}}^0 - T \Delta S_{\text{abs}}^0 \quad (3)$$

$$\ln\left(\frac{H}{P^0}\right) = \frac{-\Delta H_{\text{abs}}^0}{RT} + \frac{\Delta S_{\text{abs}}^0}{R} \quad (4)$$

The standard enthalpy and entropy of absorption ($\frac{-\Delta H_{\text{abs}}^0}{R}$ and $\frac{\Delta S_{\text{abs}}^0}{R}$) and their respective uncertainties are calculated by general uncertainty propagation for weighted least-squares linear fits according to eqs 5–8, where w is the weight and is equal to $1/\sigma(\ln H_i)^2$ and $\Delta = \sum w_i \sum w_i (1/T_i)^2 - (\sum w_i/T_i)^2$.²⁸

$$\frac{-\Delta H_{\text{abs}}^0}{R} = \frac{\sum w_i \sum w_i T_i^{-1} \ln(H_i) - \sum w_i T_i^{-1} \sum w_i \ln(H_i)}{\Delta} \quad (5)$$

$$\sigma\left(\frac{-\Delta H_{\text{abs}}^0}{R}\right) = \sqrt{\frac{\sum w_i}{\Delta}} \quad (6)$$

$$\frac{\Delta S_{\text{abs}}^0}{R} = \frac{\sum w_i (1/T_i)^2 \sum w_i \ln(H_i) - \sum w_i T_i^{-1} \sum w_i T_i^{-1} \ln(H_i)}{\Delta} \quad (7)$$

$$\sigma\left(\frac{\Delta S_{\text{abs}}^0}{R}\right) = \sqrt{\frac{\sum w_i (1/T_i)^2}{\Delta}} \quad (8)$$

4. RESULTS AND DISCUSSION

The characterization of the polymers studied in this work is reported in Table 2. The polymers have low glass transition temperatures and high decomposition temperatures, both of which are favorable for gas separation applications. Poly(ethylene oxide) was the only semicrystalline polymer studied, and it had a melting point of 294.15 K.

The polymer densities are required to perform a buoyancy correction to the gravimetric gas solubility data to account for the change in sample weight due to buoyancy forces. The polymer densities are shown in Table 3.

To validate the gravimetric apparatus, the solubility of CO₂ in PEO-0.4 was measured at 313.15 and 333.15 K and compared to the results reported by Li et al. The results are shown in Figure 2, and the measured values are shown in

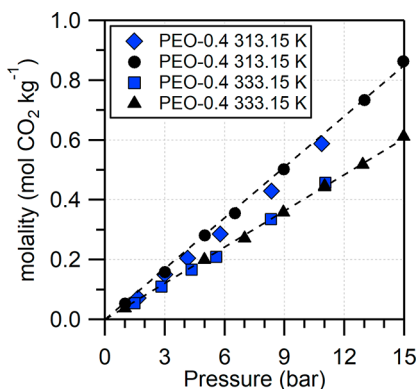


Figure 2. CO₂ solubility in PEO (moles of CO₂ per kg of polymer) at 313.15 and 333.15 K. This work, black circles and triangles; Li et al.,²⁹ blue diamonds and squares.

Table 4. The average relative deviation (ARD) between the molality measured by Li et al. and the fits to the measured data from this work are 15 and 5% for 313.15 and 333.15 K, respectively. We believe the larger deviation at 313.15 K is due to the slight deviation from linearity of the Li et al. data. The Henry's law constants at 313.15 and at 333.15 K for PEO-0.4 are 17.6 ± 0.8 and 24.8 ± 0.3 bar·kg/mol, respectively. These match the values reported by Li et al. of 19.1 ± 0.9 and 24.8 ± 1.0 bar·kg/mol for CO₂ in PEO-0.4 at 313.15 and 333.15 K, respectively,²⁹ within experimental uncertainty.

4.1. Effect of Polymer Pendant Chain Structure. The ether backbone of poly(ethylene oxide) interacts favorably

with CO₂ molecules, leading to high capacity and high selectivity for CO₂ over other gases. Because the ether linkages are known to increase CO₂ solubility,^{3–6} a series of poly(glycidyl ethers) was studied to determine the effect of the side chain structure of the poly(glycidyl ether) on CO₂ solubility. CO₂ molality as a function of pressure at room temperature and 333.15 K for four poly(glycidyl ethers) and PEO are shown in Figure 3, and the measured data are shown

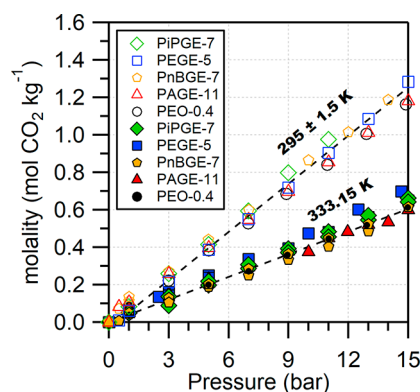


Figure 3. Solubility of CO₂ in poly(glycidyl ethers) and PEO at 295.0 ± 1.5 K (open symbols) and 333.15 ± 0.10 K (filled symbols).

in Table 4 (PEO) and Tables 5–8 for the poly(glycidyl ethers). The Henry's law constants based on molality are reported in Table 9. Surprisingly, neither the presence of a second oxygen atom per repeat unit nor side chain character has any effect on the solubility of CO₂ in the poly(glycidyl ethers). The poly(glycidyl ethers) have different molecular weights. However, the molality of CO₂ in PEO has been found to be independent of molecular weight and structure.^{13,30} Therefore, we believe it is reasonable to compare the polymers studied here despite the variations in molecular weight. The equal solubilities of CO₂ in poly(glycidyl ethers) and PEO is remarkable and supports our hypothesis that poly(glycidyl ethers) could be used as alternatives to PEO for CO₂ separation.

Another way to consider CO₂ solubility is in terms of mole fraction, x . From this perspective, it has been reported that CO₂ solubility increases with increasing molecular weight in low molecular weight polymers (and ionic liquids), despite the observation that solubilities are very similar based on molality.^{29,31,32} The uncertainty in the number average

Table 4. CO₂ Solubility in PEO-0.4, Expressed Both as Moles of CO₂ per Mole of Polymer Repeat Unit Plus CO₂ (Mole Fraction, x), and Moles of CO₂ per Kilogram of Polymer (Molality, m)^a

295 K			313.15 K			333.15 K		
P (bar)	x	m (mol kg ⁻¹)	P (bar)	x	m (mol kg ⁻¹)	P (bar)	x	m (mol kg ⁻¹)
0.00	0.000	0.00	0.00	0.000	0.00	0.00	0.000	0.00
1.00	0.003	0.08	1.00	0.002	0.05	1.01	0.002	0.04
2.99	0.010	0.22	3.00	0.007	0.16	4.98	0.009	0.20
5.00	0.017	0.38	4.99	0.012	0.28	7.00	0.012	0.27
6.99	0.023	0.53	6.51	0.015	0.36	8.94	0.016	0.36
8.89	0.029	0.68	8.96	0.022	0.50	11.01	0.019	0.44
10.93	0.036	0.84	13.01	0.031	0.73	11.01	0.019	0.45
12.91	0.042	1.01	14.95	0.037	0.86	12.93	0.022	0.52
14.87	0.049	1.16				14.97	0.026	0.61

^aStandard uncertainties are $u(x) = 0.001$, $u(m) = 0.01$ mol/kg, $u(T) = 0.1$ K except at room temperature where $u(T) = 1.5$ K, $u(P) = 0.01$ bar.

Table 5. CO₂ Solubility in PEGE-5, Expressed Both as Moles of CO₂ per Mole of Polymer Repeat Unit Plus CO₂ (Mole Fraction, x), and Moles of CO₂ per Kilogram of Polymer (Molality, m)^a

294–295.4 K			333.15 K			343.15 K		
P (bar)	x	m (mol kg ⁻¹)	P (bar)	x	m (mol kg ⁻¹)	P (bar)	x	m (mol kg ⁻¹)
0.00	0.000	0.00	0.00	0.000	0.00	0.00	0.000	0.0000
0.50	0.001	0.01	0.01	0.000	0.00	1.00	0.004	0.0402
1.00	0.006	0.06	1.00	0.006	0.05	2.99	0.012	0.1228
3.00	0.022	0.22	1.00	0.007	0.06	7.01	0.027	0.2713
5.00	0.038	0.39	2.50	0.014	0.14	11.00	0.042	0.4300
7.00	0.053	0.55	3.00	0.016	0.16	14.93	0.058	0.6058
9.00	0.068	0.72	3.00	0.014	0.14	13.02	0.050	0.5121
11.00	0.084	0.90	5.00	0.025	0.25	9.00	0.034	0.3462
13.00	0.100	1.09	5.00	0.024	0.24	5.00	0.020	0.1969
15.00	0.116	1.28	7.00	0.030	0.30			
			7.00	0.033	0.34			
			9.00	0.039	0.39			
			10.00	0.046	0.47			
			11.00	0.047	0.48			
			12.50	0.058	0.60			
			13.00	0.054	0.56			
			14.65	0.067	0.70			
			15.00	0.062	0.65			

^aStandard uncertainties are $u(x) = 0.002$, $u(m) = 0.03$ mol/kg, $u(T) = 0.1$ K, $u(P) = 0.01$ bar. $u(T) = 1.5$ K at room temperature with the range over the course of the experiments given.

Table 6. CO₂ Solubility in PAGE-11, Expressed Both as Moles of CO₂ per Mole of Polymer Repeat Unit Plus CO₂ (Mole Fraction, x), and Moles of CO₂ per Kilogram of Polymer (Molality, m)^a

294.3–295.4 K			333.15 K		
P (bar)	x	m (mol kg ⁻¹)	P (bar)	x	m (mol kg ⁻¹)
0.00	0.000	0.00	0.00	0.000	0.00
1.00	0.012	0.11	0.01	0.000	0.00
5.00	0.043	0.40	1.00	0.006	0.05
9.00	0.074	0.70	1.00	0.009	0.08
13.00	0.104	1.01	3.00	0.017	0.15
15.00	0.119	1.18	5.00	0.023	0.21
11.00	0.089	0.86	5.00	0.026	0.23
7.00	0.059	0.55	7.00	0.032	0.29
3.00	0.029	0.26	9.00	0.041	0.38
0.50	0.009	0.08	10.00	0.041	0.38
			11.00	0.049	0.45
			11.96	0.052	0.48
			13.00	0.056	0.52
			14.00	0.058	0.54
			15.00	0.064	0.60

^aStandard uncertainties are $u(x) = 0.003$, $u(m) = 0.02$ mol/kg, $u(T) = 0.1$ K, $u(P) = 0.01$ bar. $u(T) = 1.5$ K at room temperature with the range over the course of the experiments given.

molecular weights of some of the polymers investigated here is significant (i.e., see the PDI values in Table 2). Therefore, the mole fraction of CO₂ dissolved was calculated using the molecular weight of the polymer repeat unit as opposed to the number average molecular weight of the polymer. The solubility isotherms in terms of mole fraction (moles of CO₂ per mole of polymer repeat unit plus CO₂) at room temperature and 333.15 K are shown in Figure 4, and the measured data are shown in Tables 5–8. Based on the knowledge that ether linkages increase CO₂ solubility due to favorable interactions between the ether oxygen and CO₂, we

Table 7. CO₂ Solubility in PiPGE-7, Expressed Both as Moles of CO₂ per Mole of Polymer Repeat Unit Plus CO₂ (Mole Fraction, x), and Moles of CO₂ per Kilogram of Polymer (Molality, m)^a

294.4–296.2 K			333.15 K		
P (bar)	x	m (mol kg ⁻¹)	P (bar)	x	m (mol kg ⁻¹)
0.00	0.000	0.00	0.00	0.000	0.00
1.00	0.010	0.08	1.00	0.006	0.05
3.00	0.029	0.26	1.00	0.006	0.05
5.00	0.046	0.41	3.00	0.016	0.14
7.00	0.065	0.59	3.00	0.010	0.09
9.00	0.085	0.80	5.00	0.022	0.20
11.00	0.102	0.98	5.00	0.025	0.22
			7.00	0.032	0.29
			7.00	0.034	0.31
			9.00	0.044	0.39
			9.00	0.041	0.37
			11.00	0.053	0.48
			11.00	0.050	0.46
			13.00	0.060	0.55
			13.00	0.062	0.57
			15.00	0.072	0.66
			15.00	0.070	0.64

^aStandard uncertainties are $u(x) = 0.001$, $u(m) = 0.02$ mol/kg, $u(T) = 0.1$ K, $u(P) = 0.01$ bar. $u(T) = 1.5$ K at room temperature with the range over the course of the experiments given.

expected the CO₂ solubility to be directly related to the weight fraction of oxygen in the polymer repeat unit. However, the results show solubility increasing with increasing repeat unit molecular weight, regardless of the polymer structure for this series of polyethers, which is the order of decreasing oxygen weight fraction in the polymer repeat unit. Often, molar volume is used as a surrogate for free volume owing to the difficulty of measuring free volume. The direct relationship between the molecular weight of the polymer repeat unit and

Table 8. CO₂ Solubility in PnBGE-7, Expressed Both as Moles of CO₂ per Mole of Polymer Repeat Unit Plus CO₂ (Mole Fraction, x), and Moles of CO₂ per Kilogram of Polymer (Molality, m)^a

292.9–294.7 K			333.15 K		
P (bar)	x	m (mol kg ⁻¹)	P (bar)	x	m (mol kg ⁻¹)
0.00	0.000	0.00	0.00	0.000	0.00
0.50	0.009	0.07	0.50	0.001	0.01
1.00	0.015	0.11	1.00	0.006	0.04
1.00	0.017	0.14	1.00	0.006	0.05
3.00	0.034	0.27	3.00	0.017	0.13
4.99	0.054	0.44	3.00	0.014	0.11
7.02	0.072	0.60	5.00	0.024	0.19
10.00	0.101	0.86	5.00	0.026	0.20
11.99	0.117	1.01	7.00	0.032	0.25
13.99	0.134	1.19	7.00	0.036	0.28
			9.00	0.042	0.33
			9.00	0.045	0.36
			11.00	0.055	0.45
			11.00	0.050	0.40
			13.00	0.059	0.48
			13.00	0.064	0.52
			15.00	0.074	0.61

^aStandard uncertainties are $u(T) = 0.1$ K, $u(P) = 0.01$ bar, $u(x) = 0.005$ (room temperature) and 0.001 (333.15 K), $u(m) = 0.02$ mol/kg, $u(T) = 1.5$ K at room temperature with the range over the course of the experiments given.

CO₂ solubility and the indirect relationship with oxygen content suggests CO₂ solubility in these polymers is governed by free volume and not specific interactions between the gas and the polymer. The trend is preserved with increasing temperature, although it is less pronounced at 333.15 K than at room temperature. The H values calculated on the mole fraction basis are shown in Table 10 and follow the same trend, i.e., solubility increasing and H decreasing as molecular weight of the polymer repeat unit increases. The H values calculated from the data published by Li et al. for PEO-0.4, recast in terms of repeat unit molecular weight, are also included in Table 10. The uncertainties were propagated through the linear regression and are considerably higher than the values reported by Li et al.²⁹ We attribute the difference in the H values at 313.15 K from our data and those calculated from Li et al. to the previously mentioned deviation from linearity in the Li et al. data.

4.2. Thermodynamics of Gas Dissolution. As expected, the CO₂ solubility in poly(glycidyl ethers) decreases with increasing temperature, indicating favorable enthalpic interactions between the CO₂ and the polymers. As shown above, the isotherms for all poly(glycidyl ethers) and PEO at both room temperature and 333.15 K are very similar on a molality basis. However, the solubility in terms of mole fraction increases with increasing polymer repeat unit molecular

weight. On either basis, the differences in solubility between the poly(glycidyl ether) polymers is quite small; therefore, the thermodynamics of gas dissolution in all poly(glycidyl ethers) are expected to be similar.

Poly(ethyl glycidyl ether) was chosen as an example poly(glycidyl ether) to compare the thermodynamics of gas solubility to PEO. Measurements of the solubility of CO₂ in PEGE and PEO at three temperatures provides the necessary data to calculate the standard entropy and enthalpy of CO₂ absorption. The temperature dependence of solubility (mole fraction of CO₂ based on the molecular weight of the polymer repeat unit) in PEGE and PEO are shown in Figure 5, and the measured data are shown in Tables 4 and 5.

The Henry's law constants calculated based on the isotherms in Figure 4 are shown in Table 10. $\ln(H)$ vs $1/T$ values are plotted in Figure 5 along with the values reported by Li et al.²⁹ after we recast their data using moles of polymer repeat unit instead of moles of polymer. As we described above, we believe this is a more reasonable metric for comparison between polymers of different molecular weights. It is worth mentioning that the molecular weight of the PEO repeat unit is 44.05 g/mol and that of PEGE is 102.13 g/mol. A weighted least-squares linear fit to the data in Figure 6 was used to determine the enthalpy and entropy of CO₂ dissolution. The calculated enthalpy and entropy are shown in Table 11 and are compared to those calculated from the recast Henry's law constants we obtained from data reported by Li et al.²⁹

First, we note that the standard enthalpy and entropy of absorption of CO₂ in PEO from this study are quite similar to the values obtained from the Li et al.²⁹ data and agree within the estimated uncertainties. The standard enthalpy of absorption values are negative, indicating attraction between the CO₂ and the polymers. The magnitude of the ΔH^0 values are consistent with physically dissolved CO₂. The approximately equal enthalpies of absorption in PEO and PEGE suggest that there are no additional CO₂–polymer interactions per mole of repeat unit present in PEGE, despite the presence of a second ether oxygen per repeat unit. In fact, the enthalpy is slightly less favorable in PEGE than in PEO, which could suggest that the side chain hinders some CO₂–polymer interactions. Higher glass transition temperature is indicative of less chain mobility and is typically correlated with higher entropic penalty for gas dissolution. However, the entropic penalty for CO₂ dissolution in PEGE is slightly lower than that in PEO despite the higher glass transition temperature of PEGE. This could be a result of tighter packing of PEO chains because it is semicrystalline, whereas PEGE is amorphous and did not have a measurable melting point.

4.3. Effect of Replacing Ether Backbone with Vinyl Backbone while Retaining an Ether Linkage in the Pendant Chain. The equal solubility of CO₂ and standard enthalpy of absorption in poly(glycidyl ethers) and PEO

Table 9. Henry's Law Constants (H) Based on CO₂ Molality

H (bar·kg·mol ⁻¹)	295 ± 1.5 K	313.15 K	333.15 K	343.15 K
PEO-0.4	12.9 ± 0.1	17.6 ± 0.3	24.8 ± 0.3	
PEGE-5	12.1 ± 0.4		21.9 ± 1.1	25.3 ± 0.5
PAGE-11	12.7 ± 0.3		24.9 ± 1.2	
PiPGE-7	11.4 ± 0.3		23.3 ± 0.8	
PnBGE-7	11.7 ± 0.3		25.5 ± 1.0	

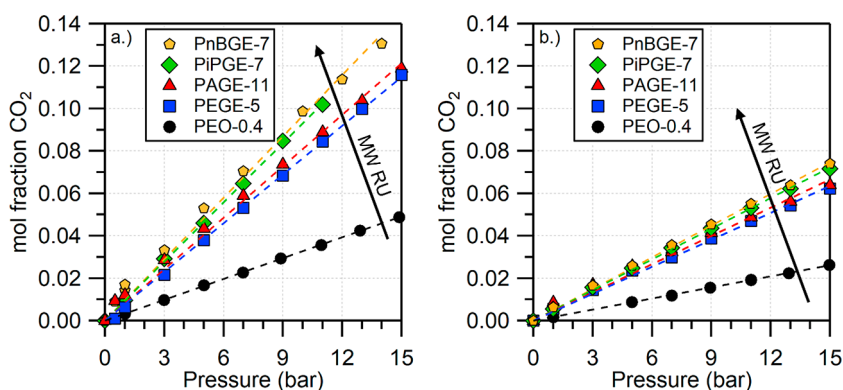


Figure 4. Mole fraction solubility of CO₂ in poly(glycidyl ethers) at (a) 295 ± 1.5 K and (b) at 333.15 ± 0.1 K compared to that in PEO-0.4 calculated based on molecular weight of the polymer repeat unit (MW RU).

Table 10. Henry's Law Constants (H) Based on CO₂ Mole Fraction (Using the Molecular Weight of the Repeat Unit of the Polymer)

H (bar)	295 ± 1.5 K	303.15 K	313.15 K	323.15 K	333.15 K	343.15 K
PEO-0.4 ^a		364 ± 16	444 ± 16	520 ± 16	572 ± 18	
PEO-0.4	305 ± 1		413 ± 4		574 ± 5	
PEGE-5	131 ± 2				226 ± 12	259 ± 4
PAGE-11	124 ± 5				230 ± 13	
PiPGE-7	107 ± 1				213 ± 7	
PnBGE-7	101 ± 5				207 ± 8	

^aValues recalculated from data reported in ref 29.

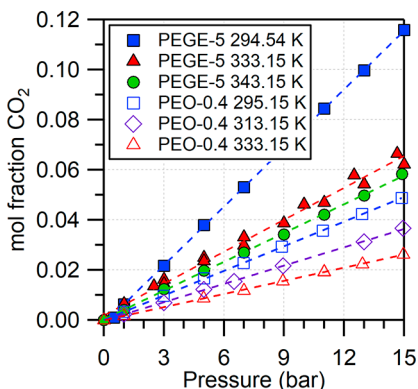


Figure 5. Temperature dependence of CO₂ solubility in PEGE and PEO. The mole fraction is calculated based on the moles of polymer repeat unit in the sample.

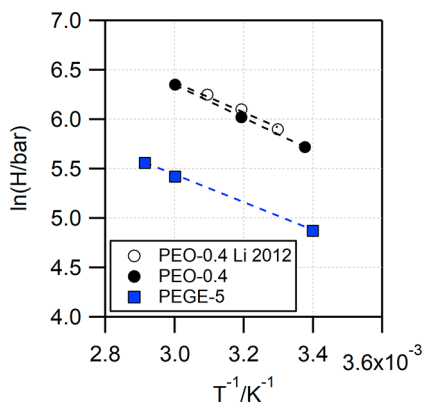


Figure 6. ln(H) vs $1/T$ plot for CO₂ dissolution in PEGE and PEO-0.4, including data reported by Li et al.²⁹

Table 11. Thermodynamic Parameters of CO₂ Dissolution in PEO and PEGE

	ΔH^0 (kJ mol ⁻¹)	ΔS^0 (J mol ⁻¹ K ⁻¹)
PEO-0.4 ^a	-12.5 ± 1.4	-90.4 ± 8.6
PEO-0.4	-14.0 ± 0.2	-95 ± 0.7
PEGE-5	-11.8 ± 0.4	-80.5 ± 1

^aValues recalculated from data reported in ref 29.

suggests that the dissolved CO₂ may only interact with only one ether oxygen in the polymer repeat unit and that no enhanced interactions are observed because the second ether oxygen is inaccessible.³³ It has been reported previously that the position of polar groups in polymers affects their solubility in supercritical CO₂.³³ We expect a similar effect on the solubility of CO₂ in polyethers based on the placement of the ether oxygen.

The effect of the position of the ether oxygen in the polymer repeat unit on CO₂ solubility was investigated by measuring the solubility of CO₂ in PEVE. PEVE has a pendant chain structure similar to that of poly(ethyl glycidyl ether) but has a vinyl-derived backbone as opposed to the ether backbone of PEO and PEGE. The only oxygen present in the repeat unit is on the pendant chain. It has also been reported that PEVE is less soluble in supercritical CO₂ than PEO, which suggests that interactions between CO₂ and PEVE are less favorable than those between CO₂ and PEO.³³ The solubility of CO₂ in PEVE in terms of molality and mole fraction is shown in Figure 7, and the measured data are shown in Table 12. The Henry's law constants calculated in terms of mole fraction and molality are shown in Table 13.

The CO₂ uptake in terms of mole fraction is lower in PEVE than in PEGE, which is consistent with the observed trend of increasing solubility with increasing polymer repeat unit

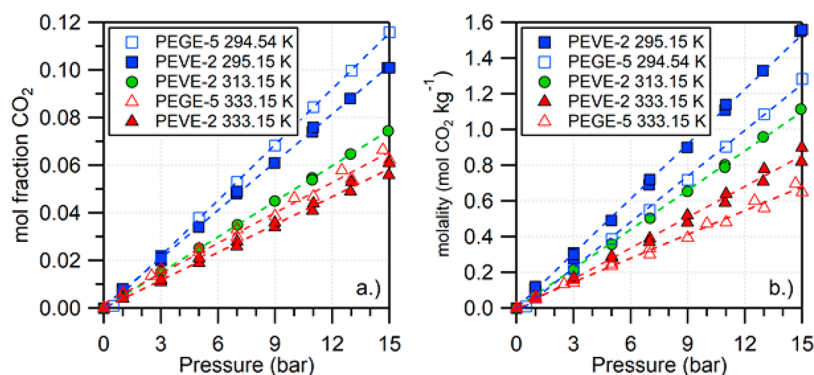


Figure 7. Solubility of CO₂ in PEVE in terms of mole fraction (a) and molality (b).

Table 12. CO₂ Solubility in PEVE-2, Expressed Both as Moles of CO₂ per Mole of Polymer Repeat Unit Plus CO₂ (Mole Fraction, x), and Moles of CO₂ per Kilogram of Polymer (Molality, m)^a

295.15 K			313.15 K			333.15 K		
P (bar)	x	m (mol kg ⁻¹)	P (bar)	x	m (mol kg ⁻¹)	P (bar)	x	m (mol kg ⁻¹)
0.00	0.000	0.00	0.00	0.000	0.00	0.00	0.000	0.00
0.98	0.007	0.09	0.99	0.005	0.07	1.00	0.004	0.05
1.00	0.007	0.10	2.99	0.015	0.21	1.00	0.004	0.05
0.98	0.008	0.11	5.00	0.025	0.36	2.99	0.011	0.16
0.99	0.008	0.12	7.01	0.035	0.50	3.00	0.012	0.17
3.00	0.020	0.28	8.97	0.045	0.65	5.00	0.019	0.28
3.00	0.020	0.28	10.94	0.055	0.80	5.00	0.021	0.29
3.00	0.022	0.31	10.94	0.054	0.79	7.00	0.028	0.39
3.00	0.021	0.30	12.95	0.065	0.96	6.98	0.026	0.37
4.99	0.034	0.49	14.93	0.074	1.12	8.98	0.034	0.48
6.97	0.048	0.69				8.98	0.036	0.52
6.99	0.049	0.72				10.96	0.041	0.59
8.96	0.061	0.90				11.00	0.044	0.64
10.95	0.074	1.11				13.00	0.053	0.78
10.99	0.076	1.14				12.96	0.049	0.71
12.94	0.088	1.33				14.96	0.056	0.82
14.89	0.101	1.55				14.99	0.061	0.90
15.00	0.101	1.56						

^aStandard uncertainties are $u(x) = 0.001$, $u(m) = 0.02$ mol/kg, $u(T) = 0.1$ K, $u(P) = 0.01$ bar.

Table 13. Henry's Law Constants (H) for PEVE

	295.15 K	313.15 K	333.15 K
H (bar·kg·mol ⁻¹)	9.7 ± 0.2	13.6 ± 0.2	17.6 ± 0.7
H (bar)	147 ± 2	201 ± 1	256 ± 10

molecular weight. The standard enthalpy and entropy of absorption in PEVE are -12.9 ± 0.4 kJ mol⁻¹ and -85.3 ± 1 J mol⁻¹K⁻¹, respectively. The standard enthalpy of CO₂ dissolution in PEVE is not significantly lower than that in PEGE. However, the entropic penalty is greater for CO₂ dissolution in PEVE than in PEGE, which is consistent with the higher glass transition temperature of PEVE compared to PEGE. Thus, we conclude that CO₂ is able to interact with pendant chain ether oxygens as well as it can with backbone ether oxygens. However, the presence of ether oxygens in both the backbone and the pendant chain (i.e., PEGE, PAGE, PiPGE, and PnBGE) does not significantly enhance CO₂ dissolutions.

4.4. Polymer Viscosity. Viscosity is an important physicochemical property to consider in the design of liquid absorbents for gas separation because it affects the rate of mass transfer of gas into the solvent. The temperature-dependent

viscosities of the polymers studied in this work are shown in Figure 8, and the measured data are shown in Tables 14 and S5.

The viscosities of PEGE-5, PAGE-11, and PnBGE-7 were measured on the Brookfield CAP2000 cone and plate viscometer. At each temperature, the viscosity was measured

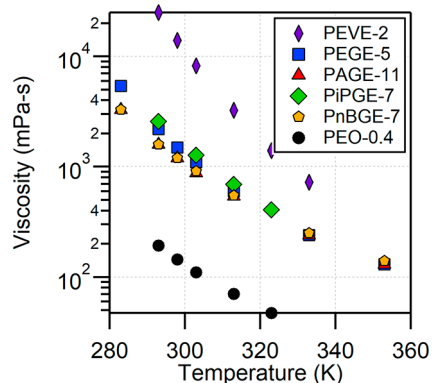


Figure 8. Temperature-dependent viscosity of polyethers.

Table 14. Temperature-Dependent Dynamic Viscosity (μ) for PEO-0.4, Poly(glycidyl ethers), and PEVE-2^a

T (K)	μ (mPa·s)	shear rate (s ⁻¹)	T (K)	μ (mPa·s)	shear rate (s ⁻¹)	T (K)	μ (mPa·s)	shear rate (s ⁻¹)
PEO-0.4			PiPGE-7			PnBGE-7		
293.15	193		293.15	2580	4.06	283.15	3300	— ^b
298.15	144		303.15	1270	7.9	293.15	1600	— ^b
303.15	110		313.15	693	13.8	298.15	1200	— ^b
313.15	70.3		323.15	408	22.3	303.15	910	— ^b
323.15	47.2					313.15	550	— ^b
						333.15	250	— ^b
						353.15	140	— ^b
PEGE-5			PAGE-10			PEVE-2		
283.15	5400	— ^b	283.15	3300	— ^b	293.15	25000	40
293.15	2200	— ^b	293.15	1600	— ^b	298.15	14000	67
298.15	1500	— ^b	298.15	1200	— ^b	303.15	8250	117
303.15	1100	— ^b	303.15	880	— ^b	313.15	3250	316
313.15	600	— ^b	313.15	540	— ^b	323.15	1400	667
333.15	240	— ^b	333.15	240	— ^b	333.15	725	1333
353.15	130	— ^b	353.15	130	— ^b			

^aStandard uncertainties are $u(\mu) = \pm 0.5\%$ and $u(T) = \pm 0.02$ K for PEO-0.4 (rolling ball viscometer) and PiPGE-7 (SVM 2001) and $u(\mu) = \pm 7\%$ and $u(T) = \pm 0.1$ K for all other polymers (Brookfield CAP2000). ^bValue is the average of three shear rates shown in the Supporting Information.

at three shear rates. The standard deviation of viscosity obtained at different shear rates was less than 0.5% for all polymers (significantly lower than the uncertainty of the measurement, 7%). Therefore, the viscosities of PEGE-5, PAGE-11, and PnBGE-7 were considered independent of shear rate, and the average values are shown in Figure 8. Due to the similar viscosity and structure of PiPGE, its viscosity was also considered independent of shear rate. Its viscosity was measured using the Anton Paar SVM 2001, which automatically selects the shear rate. The viscosity and the shear rate at which it was measured are shown in Table 14. Barteau measured the viscosity of these four poly(glycidyl ethers) and obtained the following values for zero-shear viscosity at (297 K): PAGE 3.2 Pa·s, PEGE 2.2 Pa·s, PiPGE 3.4 Pa·s, and PnBGE 1.8 Pa·s.³⁴ The viscosities reported here are of the same order of magnitude but are considerably lower due to the lower molecular weight of the polymers used in this work (5–10 kg/mol) compared to those studied previously (22–25 kg/mol). The viscosity of PEO-0.4 was measured in the Anton Paar Lovis 2000 M/ME rolling ball viscometer. The values we report are higher than those reported by Ottani et al. in 2002.³⁵ The deviation could be caused by slight differences in molecular weight as well as polymer water content. Ottani et al. report that the polymers were used without further purification. Here, the polymers were dried for 2 days at 333 K to remove volatile impurities before viscosity measurement. The water content of PEO-0.4 measured by Karl Fischer titration directly before the viscosity measurement was 1000 ppm in this work. The viscosity of PEVE-2 is considerably higher than the poly(ethers) owing to its more rigid vinyl backbone. Based on these measurements PEO-0.4, which has the lowest molecular weight and therefore the lowest viscosity, would be the most promising absorbent. However, the viscosities of the other polymers could be reduced by decreasing the number-average molecular weight without impacting the CO₂ solubility in terms of molality. Another alternative would be the development of poly(glycidylether) polymeric membranes for gas separation.

5. CONCLUSIONS

The solubility of CO₂ in four poly(glycidyl ethers) was measured at multiple temperatures. At both room temperature and 333.15 K, the solubility of CO₂ in molality units in all poly(glycidyl ethers) and PEO were essentially equal. As the molecular weight of the polymer repeat unit increases, the CO₂ solubility in terms of mole fraction increases, regardless of the polymer structure. The CO₂ solubility in PEVE, which does not have an ether in the polymer backbone, followed the same CO₂ solubility trend as the other polymers in terms of mole fraction. The application of poly(glycidyl ethers) as alternatives to PEO will depend on the enthalpy and entropy of absorption in addition to the solubility. The standard enthalpy of CO₂ dissolution was very similar in PEGE and PEO. Unexpectedly, the thermodynamics of CO₂ dissolution were virtually unaffected by ether oxygen placement; the standard enthalpies of CO₂ dissolution in PEGE and PEVE were not significantly different. Because poly(glycidyl ethers) and poly(ethyl vinyl ether) are noncrystalline (thus, not limiting the useful molecular weight range) and hydrophobic, yet have capacities and standard enthalpies for CO₂ absorption similar to those of PEO, we conclude that they could be effective alternatives to PEO for CO₂ separations.

■ ASSOCIATED CONTENT

Supporting Information

The Supporting Information is available free of charge at <https://pubs.acs.org/doi/10.1021/acs.jced.1c00219>.

¹H NMR spectra used to estimate polymer purity, polymer characterization, including GPC, DSC, TGA, and density, a discussion of the buoyancy correction for the gravimetric technique and the calculation of sample density by gravimetric analysis, and finally, a discussion of the estimation of uncertainty in the density measurements and the impact of uncertainty in density on the calculation of Henry's law constants (PDF)

AUTHOR INFORMATION

Corresponding Authors

Joan F. Brennecke – McKetta Department of Chemical Engineering, University of Texas at Austin, Austin, Texas 78712, United States; orcid.org/0000-0002-7935-2134; Email: jfb@che.utexas.edu

Nathaniel A. Lynd – McKetta Department of Chemical Engineering, University of Texas at Austin, Austin, Texas 78712, United States; orcid.org/0000-0003-3010-5068; Email: lynd@che.utexas.edu

Authors

Caitlin L. Bentley – McKetta Department of Chemical Engineering, University of Texas at Austin, Austin, Texas 78712, United States; orcid.org/0000-0003-2965-9768

Tangqiumei Song – McKetta Department of Chemical Engineering, University of Texas at Austin, Austin, Texas 78712, United States

Benjamin J. Pedretti – McKetta Department of Chemical Engineering, University of Texas at Austin, Austin, Texas 78712, United States

Michael J. Lubben – McKetta Department of Chemical Engineering, University of Texas at Austin, Austin, Texas 78712, United States

Complete contact information is available at:
<https://pubs.acs.org/10.1021/acs.jced.1c00219>

Notes

The authors declare no competing financial interest.

ACKNOWLEDGMENTS

This research was funded by the Robert A. Welch Foundation (Grant F-1945) and the National Science Foundation (CBET-1706968).

REFERENCES

- (1) Nexant Incorporated. *Equipment Design and Cost Estimation for Small Modular Biomass Systems, Synthesis Gas Cleanup, and Oxygen Separation Equipment Task 2.3: Sulfur Primer*; National Renewable Energy Laboratory, 2006.
- (2) Brinkmann, T.; Lillepär, J.; Notzke, H.; Pohlmann, J.; Shishatskiy, S.; Wind, J.; Wolff, T. Development of CO₂ Selective Poly(Ethylene Oxide)-Based Membranes: From Laboratory to Pilot Plant Scale. *Eng.* **2017**, *3* (4), 485–493.
- (3) Lin, H.; Freeman, B. D. Gas and Vapor Solubility in Cross-Linked Poly(ethylene Glycol Diacrylate). *Macromolecules* **2005**, *38*, 8394–8407.
- (4) Lin, H.; Freeman, B. D. Gas solubility, diffusivity and permeability in poly(ethylene oxide). *J. Membr. Sci.* **2004**, *239*, 105–117.
- (5) Hirayama, Y.; Kase, Y.; Tanihara, N.; Sumiyama, Y.; Kusuki, Y.; Haraya, K. Permeation properties to CO₂ and N₂ of poly(ethylene oxide)-containing and crosslinked polymer films. *J. Membr. Sci.* **1999**, *160* (1), 87–99.
- (6) Wang, S.; Li, X.; Wu, H.; Tian, Z.; Xin, Q.; He, G.; Peng, D.; Chen, S.; Yin, Y.; Jiang, Z.; Guiver, M. D. Advances in high permeability polymer-based membrane materials for CO₂ separations. *Energy Environ. Sci.* **2016**, *9*, 1863–1890.
- (7) Membrane Technology and Research. <https://www.mtrinc.com/our-business/refinery-and-syngas/co2-removal-from-syngas/> (May 14, 2020).
- (8) Lin, H.; Freeman, B. D. Materials selection guidelines for membranes that remove CO₂ from gas mixtures. *J. Mol. Struct.* **2005**, *739* (1–3), 57–74.

(9) Patel, N. P.; Hunt, M. A.; Lin-Gibson, S.; Bencherif, S.; Spontak, R. J. Tunable CO₂ transport through mixed polyether membranes. *J. Membr. Sci.* **2005**, *251*, 51–57.

(10) Li, J.; You, C.; Chen, L.; Ye, Y.; Qi, Z.; Sundmacher, K. Dynamics of CO₂ Absorption and Desorption Processes in Alkanolamine with Cosolvent Polyethylene Glycol. *Ind. Eng. Chem. Res.* **2012**, *51*, 12081–12088.

(11) Zhang, B.; Bogush, A.; Wei, J.; Zhang, T.; Hu, J.; Li, F.; Yu, Q. Reversible Carbon Dioxide Capture at High Temperatures by Tetraethylenepentamine Acetic Acid and Polyethylene Glycol Mixtures with High Capacity and Low Viscosity. *Energy Fuels* **2017**, *31*, 4237–4244.

(12) Usman, M.; Huang, H.; Li, J.; Hillestad, M.; Deng, L. Optimization and Characterization of an Amino Acid Ionic Liquid and Polyethylene Glycol Blend Solvent for Precombustion CO₂ Capture: Experiments and Model Fitting. *Ind. Eng. Chem. Res.* **2016**, *55*, 12080–12090.

(13) Aionicesei, E.; Škerget, M.; Knez, Ž. Measurement and Modeling of the CO₂ solubility in Poly(ethylene glycol) of different Molecular Weights. *J. Chem. Eng. Data* **2008**, *53*, 185–188.

(14) Olivieri, L.; Tena, A.; De Angelis, M. G.; Giménez, A. H.; Lozano, A. E.; Sarti, G. C. The effect of humidity on the CO₂/N₂ separation performance of copolymers based on hard polyimide segments and soft polyether chains: Experimental and modeling. *Green Energy Environ.* **2016**, *1* (3), 201–210.

(15) Hong, B.; Panagiotopoulos, A. Z. Atomistic simulation of CO₂ solubility in poly(ethylene oxide) oligomers. *Mol. Phys.* **2014**, *112* (11), 1540–1547.

(16) Lin, H.; Kai, T.; Freeman, B. D.; Kalakkunnath, S.; Kalika, D. The Effect of Cross-Linking on Gas Permeability in Cross-Linked Poly(Ethylene Glycol Diacrylate). *Macromolecules* **2005**, *38*, 8381–8393.

(17) Kusuma, V. A.; Macala, M. K.; Baker, J. S.; Hopkinson, D. Cross-linked poly(ethylene oxide) Ion Gels Containing Functionalized Imidazolium Ionic Liquids as Carbon Dioxide Separation Membranes. *Ind. Eng. Chem. Res.* **2018**, *57* (34), 11658–11667.

(18) Kusuma, V. A.; Macala, M. K.; Liu, J.; Marti, A. M.; Hirsch, R. J.; Hill, L. J.; Hopkinson, D. Ionic liquid compatibility in polyethylene oxide/siloxane ion gel membranes. *J. Membr. Sci.* **2018**, *545*, 292–300.

(19) Patel, N. P.; Miller, A. C.; Spontak, R. J. Highly CO₂-Permeable and-Selective Membranes Derived from Crosslinked Poly(ethylene glycol) and Its Nanocomposites. *Adv. Funct. Mater.* **2004**, *14* (7), 699–707.

(20) Rodriguez, C. G.; Chwatko, M.; Park, J.; Bentley, C. L.; Freeman, B. D.; Lynd, N. A. Compositionally Controlled Polyether Membranes via Mono(μ alkoxo)bis(alkylaluminum)-Initiated Chain-Growth Network Epoxide Polymerization: Synthesis and Transport Properties. *Macromolecules* **2020**, *53*, 1191–1198.

(21) Lee, B. F.; Kade, M. J.; Chute, J. A.; Gupta, N.; Campos, L. M.; Fredrickson, G. H.; Kramer, E. J.; Lynd, N. A.; Hawker, C. J. Poly(allyl glycidyl ether)-A versatile and functional polyether platform. *J. Polym. Sci., Part A: Polym. Chem.* **2011**, *49* (20), 4498–4504.

(22) Lee, B. F.; Wolffs, M.; Delaney, K. T.; Sprafke, J. K.; Leibfarth, F. A.; Hawker, C. J.; Lynd, N. A. Reactivity Ratios and Mechanistic Insight for Anionic Ring-Opening Copolymerization of Epoxides. *Macromolecules* **2012**, *45* (9), 3722–3731.

(23) Bentley, C. L.; Chwatko, M.; Wheatle, B. K.; Burkey, A. A.; Helenic, A.; Morales-Collazo, O.; Ganesan, V.; Lynd, N. A.; Brennecke, J. F. Modes of interaction in binary blends of hydrophobic polyethers and imidazolium bis(trifluoromethylsulfonyl)imide ionic liquids. *Macromolecules* **2020**, *53*, 6519.

(24) Song, T. *Gas Solubility in Ionic Liquids: Applications for Carbon Capture and Energy*. Ph.D. Thesis, University of Notre Dame.

(25) Anthony, J. L.; Maginn, E. J.; Brennecke, J. F. Solution thermodynamics of imidazolium-based ionic liquids and water. *J. Phys. Chem. B* **2001**, *105* (44), 10942–10949.

(26) Macedonia, M. D.; Moore, D. D.; Maginn, E. J.; Olken, M. M. Adsorption studies of methane, ethane, and argon in the zeolite mordenite: molecular simulations and experiments. *Langmuir* **2000**, *16* (8), 3823–3834.

(27) Chirico, R. D.; Frenkel, M.; Magee, J. W.; Diky, V.; Muzny, C. D.; Kazakov, A. F.; Kroenlein, K.; Abdulagatov, I.; Hardin, G. R.; Acree, J.; Willam, E.; Brennecke, J. F.; Brown, P. L.; Cummings, P. T.; de Loos, T. W.; Friend, D. G.; Goodwin, A. R. H.; Hansen, L. D.; Haynes, W. M.; Koga, N.; Mandelis, A.; Marsh, K. N.; Mathias, P. M.; McCabe, C.; O'Connell, J. P.; Pádua, A.; Rives, V.; Schick, C.; Trusler, J. P. M.; Vyazovkin, S.; Weir, R. D.; Wu, J. Improvement of Quality in Publication of Experimental Thermophysical Property Data: Challenges, Assessment Tools, Global Implementation, and Online Support. *J. Chem. Eng. Data* **2013**, *58*, 2699–2716.

(28) Taylor, J. R. *An Introduction to Error Analysis*, 2nd ed.; University Science Books: Sausalito, CA, 1997.

(29) Li, J.; Ye, Y.; Chen, L.; Qi, Z. Solubilities of CO₂ in Poly(ethylene glycols) from (303.15 to 333.15) K. *J. Chem. Eng. Data* **2012**, *57* (2), 610–616.

(30) Weidner, E.; Wiesmet, V.; Knez, Ž.; Škerget, M. Phase equilibrium (solid-liquid-gas) in polyethyleneglycol-carbon dioxide systems. *J. Supercrit. Fluids* **1997**, *10*, 139–147.

(31) Blath, J.; Christ, M.; Deubler, N.; Hirth, T.; Schiestel, T. Gas solubilities in room temperature ionic liquids-Correlation between RTiL-molar mass and Henry's law constant. *Chem. Eng. J.* **2011**, *172*, 167–176.

(32) Carvalho, P. J.; Coutinho, J. A. P. On the Nonideality of CO₂ Solutions in Ionic Liquids and Other Low Volatile Solvents. *J. Phys. Chem. Lett.* **2010**, *1*, 774–780.

(33) Drohmann, C.; Beckman, E. J. Phase behavior of polymers containing ether groups in carbon dioxide. *J. Supercrit. Fluids* **2002**, *22*, 103–110.

(34) Barteau, K. P. *Poly(Glycidyl Ether)-Based Battery Electrolytes: Correlating Polymer Properties to Ion Transport*; University of California Santa Barbara and ProQuest LLC, 2015.

(35) Ottani, S.; Vitalini, D.; Comelli, F.; Castellari, C. Densities, Viscosities and Refractive Indices of Poly(ethylene glycol) 200 and 400 + Cyclic Ethers at 303.15 K. *J. Chem. Eng. Data* **2002**, *47*, 1197–1204.